University of Reading

A time-domain probe method for three-dimensional rough surface reconstructions

Article

Accepted Version

Burkard, C. and Potthast, R. (2009) A time-domain probe method for three-dimensional rough surface reconstructions. Inverse problems and imaging, 3 (2). pp. 259-274. ISSN 1930-8337 doi: https://doi.org/10.3934/ipi.2009.3.259 Available at https://centaur.reading.ac.uk/29174/

It is advisable to refer to the publisher's version if you intend to cite from the work. See Guidance on citing.

To link to this article DOI: http://dx.doi.org/10.3934/ipi.2009.3.259

Publisher: American Institute of Mathematical Sciences

All outputs in CentAUR are protected by Intellectual Property Rights law, including copyright law. Copyright and IPR is retained by the creators or other copyright holders. Terms and conditions for use of this material are defined in the End User Agreement.

www.reading.ac.uk/centaur

CentAUR

Central Archive at the University of Reading

Reading's research outputs online

A Time-Domain Probe Method for Three-dimensional Rough Surface Reconstructions

C. Burkard and R. Potthast

Department of Mathematics, University of Reading
c.b.burkard@reading.ac.uk, r.w.e.potthast@reading.ac.uk

Abstract

The task of this paper is to develop a Time-Domain Probe Method for the reconstruction of impenetrable scatterers. The basic idea of the method is to use pulses in the time domain and the time-dependent response of the scatterer to reconstruct its location and shape. The method is based on the basic causality principle of time-dependent scattering. The method is independent of the boundary condition and is applicable for limited aperture scattering data.

In particular, we discuss the reconstruction of the shape of a rough surface in three dimensions from time-domain measurements of the scattered field. In practise, measurement data is collected where the incident field is given by a pulse. We formulate the time-domain field reconstruction problem equivalently via frequency-domain integral equations or via a retarded boundary integral equation based on results of Bamberger, Ha-Duong, Lubich. In contrast to pure frequency domain methods here we use a time-domain characterization of the unknown shape for its reconstruction.

Our paper will describe the Time-Domain Probe Method and relate it to previous frequency-domain approaches on sampling and probe methods by Colton, Kirsch, Ikehata, Potthast, Luke, Sylvester et al. The approach significantly extends recent work of Chandler-Wilde and Lines (2005) and Luke and Potthast (2006) on the time-domain point source method. We provide a complete convergence analysis for the method for the rough surface scattering case and provide numerical simulations and examples.

1 Introduction

We consider the scattering of a time-dependent pulse from a rough surface in three dimensions. It is usually easy to send waves into some area of the earth or the human body and measure their scattered field. The task of inverse scattering theory is to explore or visualize the structure of the unknown region and to evaluate its properties. This includes localization and shape reconstruction of the objects and interfaces and the determination of material parameters like density, conductivity or permittivity.

A *rough surface* denotes a surface which is usually a non-local perturbation of an infinite flat surface such that the surface lies within a finite distance of the original plane. In particular, we expect the rough scattering surface Γ to be the graph of some bounded continuous function $f : \mathbb{R}^2 \to \mathbb{R}$, i.e.

$$\Gamma := \left\{ x = (x_1, x_2, x_3) \in \mathbb{R}^3 : x_3 = f(x_1, x_2) \right\} . \tag{1}$$

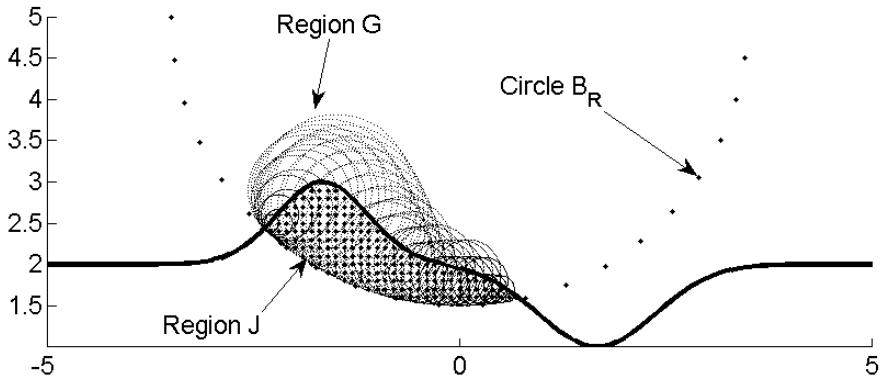

Figure 1: Basic setup for the Time-Domain Probe Method. A time-dependent pulse at some time T is indicated by the dotted circle B_R. The pulse hits the surface and generates scattered pulses, here filling the region G. The basic idea of the Time-Domain Probe Method is to mark the points x on ∂B_R where the modulus of the time-domain scattered field $U^s(x,T)$ are positive in some set $(T, T+\epsilon)$ for some $\epsilon > 0$. All these points will then be on the unknown surface Γ. Reconstructions of $U^s(x,t)$ can be carried out by the time-domain point source method [3] or the potential method [1].

Our goal is the reconstruction of the shape of the surface by given measurements in time. To this end, we describe the problem settings in the time-domain and its relation to the frequency-domain settings.

Frequency-domain problems are widely studied, for the rough surface case we refer to [4], [5], [6], [8], [9], [10], [11], [12]. There exist many methods to solve the inverse problem, most of which have been worked out for the bounded obstacle case. For example, iterative methods update some reconstruction using gradients or the Fréchet derivative with respect to the unknown boundaries [7], [26], [13]. The Point Source Method [3] and the Kirsch-Kress Method [13] reconstruct the full field and then use the boundary condition to find the unknown shape. Probe Methods as introduced by Ikehata, [20], Potthast, Nakamura and others, compare [30], usually define some indicator function via particular incident fields which can be used to construct or visualize the unknown shapes or objects. As examples for further approaches we name Sampling Methods, [14], [31], Range Tests, [21], [29], and Factorization Methods, [22], a survey is given in [30] and in [27].

The inverse rough surface problem in two dimension in the frequency domain is for example discussed by DeSanto and Wombell, [16], [17], and for the periodic case by Elschner and Yamamoto, [18]. The three-dimensional rough surface case for a single frequency is worked out in [1]. For the numerical realization of the rough surface case we employ the multi-section approach presented by Heinemeyer, Lindner, Potthast, [19].

In acoustic applications time-domain measurements are usually relatively easy to obtain whereas pure frequency domain methods do not take the full advantage of the data which are available. Here we suggest a method taking full time-measurements into account.

It is a significant step forward compared to earlier work by Chandler-Wilde and Lines [3] and by Luke and Potthast [25]. The Time-Domain Probe Method is a full time-domain scheme: it is based on causality which cannot be directly used in the frequency domain. Thus, it naturally incorporates the knowledge of scattered fields for many frequencies.

The method can be seen as an extension of the probing methods of Ikehata, Potthast, Nakamura, Sini and others. Our approach here will not rely on a particular probe in the time domain, but will in principle work with a large variety of incident time-dependent fields. In particular, the probing fields here do not need to have a singularity of any type. This avoids numerical instabilities which is one of the key problems for the realization of the time-domain probe schemes. In contrast to engineering schemes from travel-time tomography here we use a full reconstruction of the time-dependent scattered field U^s which is exploited for reconstructing the unknown surfaces.

As a part of the probing procedure we employ the time-domain field reconstruction problem by frequency-domain inverse methods and Fast Fourier Transform (FFT) via a single layer potential approach as first used by Kirsch and Kress in 1986, [13]. An alternative has been developed with the Point Source method by Chandler-Wilde and Lines, [3]. Here, we need to employ the Dirichlet Green's function for the half-space instead of the standard free-space fundamental solution for the Helmholtz equation as it has been carried out for the forward problem, [4], [5].

For the time-domain probe method the actual boundary condition is not explicitly used in the reconstruction algorithm. All arguments will be analogous for other type of boundary conditions. Thus, we expect the method to be independent of the particular physical nature of the object under consideration. Here, we will only investigate the case of the Dirichlet boundary condition in detail and leave other boundary conditions to future research.

Our presentation plan is as follows. In Section 2 we study the time-domain scattering problem and describe the retarded potential boundary integral equation which is often used to model and simulate the scattering process. Section 3 serves to summarize results about the frequency-domain scattering problem from [4], [5], [6], [8], [9], [10]. In Section 4, we present the Time-Domain Probe Method and in Section 5 we analyse its convergence. Section 6 shows numerical results for the rough surface problem.

Notation. In the following x, y, z denote points in $\mathbb{R}^3$ with coordinates (x_1, x_2, x_3), (y_1, y_2, y_3) and (z_1, z_2, z_3). Usually the reflection of these points on the x, y-plane is denoted by x', y', z' as abbreviation for $(x_1, x_2, -x_3)$, $(y_1, y_2, -y_3)$ and $(z_1, z_2, -z_3)$. The orthogonal projection of a point $x \in \mathbb{R}^3$ onto $\mathbb{R}^2$, namely (x_1, x_2), will be abreviated by a bold printed letter $\boldsymbol{x}$.

For $0 < \beta \leq 1$, let $BC^{1,\beta}(\mathbb{R}^2)$ denote the set of those bounded continuous functions $f : \mathbb{R}^2 \to \mathbb{R}$ whose gradients are bounded and uniformly Hölder continuous with index $\beta > 0$. We require that the scattering surface Γ is the graph of a function $f \in BC^{1,\beta}(\mathbb{R}^2)$ which is bounded by two constants $f_-, f_+ > 0$ such that

$$f_- < f(x_1, x_2) < f_+$$

holds for every $(x_1, x_2) \in \mathbb{R}^2$. We assume that there exists $C > f_-$ with

$$\|f\|_{BC^{1,\beta}(\mathbb{R}^2)} \leq C$$

and that our surfaces Γ can be represented as

$$\Gamma = \Gamma_f = \left\{ x \in \mathbb{R}^3 : x_3 = f(x_1, x_2) \text{ where } f \in BC^{1,\beta}(\mathbb{R}^2) \right\} . \tag{2}$$

The domain of propagation is given by

$$\Omega := \left\{ x \in \mathbb{R}^3 : x_3 > f(x_1, x_2) \right\} . \tag{3}$$

To indicate the dependence on f we also use the notation Ω_f and note that $\Gamma = \partial\Omega$.

2 The Time-Domain Problem

Let $\sigma > 0$ a constant controlling the temporal distribution of a time-dependent pulse. We study the scattering of a pulse given by

$$U^i(x,t) = \mathcal{F}\Big(\Phi(x,z,\cdot)g(\cdot)\Big)(t), \quad t \in \mathbb{R} \tag{4}$$

on a rough surface with the free-space fundamental solution

$$\Phi(x,y,\kappa) := \frac{1}{4\pi} \frac{e^{i\kappa|x-y|}}{|x-y|} , \quad x, y \in \mathbb{R}^3,\ x \neq y, \tag{5}$$

where we assume that g is chosen such that $U^i(x,t)$ is compactly supported and C^3-smooth with respect to time. Here, we consider the Fourier transform $\mathcal{F}$ with respect to frequency or time, respectively, using capital letters for the time-dependent fields and small letters in the frequency domain, i.e. we define

$$v(x,\kappa) := (\mathcal{F}V(x,\cdot))(\kappa) = \int_{-\infty}^{\infty} e^{is\kappa} V(x,s)\, ds , \quad x \in \Omega \tag{6}$$

and thus have

$$V(x,t) := (\mathcal{F}^{-1}v(x,\cdot))(t) , \quad x \in \Omega,\ t \in \mathbb{R}.$$

Throughout this paper we set the wave speed equal to one. We formulate the time-domain problem as follows.

Problem 1 (The Direct Problem in Time-Domain)**.** *Given an incident pulse $U^i(x,z,t)$ which is C^3-smooth and compactly supported with respect to time, find a solution $U^s \in H^2_{loc}(\Omega) \times (C^3(\mathbb{R}) \cap L^2(\mathbb{R}))$ of*

$$\Delta U^s(x,t) - \frac{\partial^2}{\partial t^2} U^s(x,t) = 0 , \quad x \in \Omega,\ t \in \mathbb{R} \tag{7}$$

$$U^s(x,t) = -U^i(x,t) , \quad x \in \Gamma,\ t \in \mathbb{R}. \tag{8}$$

We assume that the Fourier transform $u^s(x,\kappa)$ *of* $U^s(x,t)$ *uniformly satisfies the* boundedness condition *(compare [4])*

$$|u^s(x,\kappa)| \le c\,, \quad x \in \Omega, \tag{9}$$

with some constant c *for any fixed* κ, $\Im(\kappa) \ge 0$, *and we demand* u^s *to satisfy a* limiting absorption principle *(see (19)).*

Taking the Fourier transform with respect to time on both sides of the wave equation (7) we obtain the Helmholtz equation

$$\Delta u^s + \kappa^2 u^s = 0. \tag{10}$$

and we observe

$$(\mathcal{F}U^i(x,\cdot))(\kappa) \;=\; \Phi(x,z,\kappa)(\mathcal{F}g)(\kappa)\,, \quad x \in \Omega. \tag{11}$$

Under the above conditions we obtain uniqueness and solvability of the time-domain problem by combining uniqueness and solvability of the frequency problems and the bounds on the inverse as worked out in [5] by an application of the Fourier transform.

For a real-valued mapping $U : \Omega \times \mathbb{R} \to \mathbb{R}$ it holds that $(\mathcal{F}U(x,\cdot))(\kappa) = \overline{(\mathcal{F}U(x,\cdot))(-\kappa)}$. Further, in three-dimensions (in contrast to the two-dimensional case) there are no difficulties arising at $\kappa = 0$ as the fundamental solution $\Phi(x,y,\kappa)$ has no singularity in $\kappa = 0$ and in the following we can assume that $\kappa \in \mathbb{R}$.

Often, time-domain solutions to scattering problems are represented by time-domain integral equations [2, 24, 15]. Let Γ^* be some surface with $\Gamma^* \subset \overline{\Omega}$. By an application of the Fourier Transform to a single-layer potential representation in the frequency domain, every solution of Problem 1 which allows such a representation for allmost all wave numbers κ with a density which is in $L^2(\mathbb{R})$ with respect to the wave number can be represented as a potential

$$\begin{aligned} U^s(x,t) &= \frac{1}{4\pi}\int_{-\infty}^{\infty}\int_{\Gamma^*}\left(\frac{\delta(t-s-|x-y|)}{|x-y|} - \frac{\delta(t-s-|x-y'|)}{|x-y'|}\right)\varphi(y,s)\,ds(y)\,ds \\ &= \int_{\Gamma^*}\left(\frac{\varphi(y,t-|x-y|)}{|x-y|} - \frac{\varphi(y',t-|x-y'|)}{|x-y'|}\right)ds(y) \quad , x \in \Omega, t \in \mathbb{R}. \end{aligned} \tag{12}$$

For the limit x approaching the boundary we derive that any density φ of the above representation must satisfy the boundary integral equation

$$\mathcal{S}\varphi = U^s|_{\Gamma^*}, \tag{13}$$

where we define

$$(\mathcal{S}\varphi)(x,t) := \frac{1}{4\pi}\int_{\Gamma^*}\left(\frac{\varphi(y,t-|x-y|)}{|x-y|} - \frac{\varphi(y',t-|x-y'|)}{|x-y'|}\right)ds(y) \tag{14}$$

for $x \in \Gamma\,, t \in \mathbb{R}$. The potential

$$\mathcal{R}\varphi(x,t) := \int_{\Gamma^*} \frac{\varphi(y, t-|x-y|)}{|x-y|}\, ds(y) \tag{15}$$

is known as *retarded potential*. For a investigation of numerical methods to solve the retarded boundary integral equation for bounded surfaces, i.e. $\Gamma^* = \partial\Omega$ where Ω is a bounded subset of $\mathbb{R}^3$, we refer for example to [15]. A complete theoretical background using Laplace transforms can be found in [2] and in [24].

Here, for simulation and inversion we employ calculations using FFT and frequency domain methods. An application of the FFT with respect to time to equation (13) leads to the standard single-layer boundary integral equation in the frequency domain for all frequencies $\kappa \in \mathbb{R}$. We solve this problem for κ in a uniform grid of points and employ the inverse FFT to obtain an approximate solution to the retarded integral equation. For more details about equivalence and estimates we refer to the arguments worked out in [25]. We also refer to [28] where this equivalence has been used to construct a time-domain filter for field reconstruction from a family of frequency-domain filters. In the next section we summarize some relevant results on the frequency problem for the rough surface setting.

3 The Direct Scattering Problem in the Frequency Domain

In the frequency domain problem we consider the scattering of an acoustic field from the rough surface Γ. The incident field is due to a point source in $z \in \mathbb{R}^3$ defined by $u^i(x,\kappa) = \Phi(x,z,\kappa)$, where Φ is the fundamental solution of the Helmholtz equation (5). As we have seen we can limit our attention to the case $\kappa \geq 0$. The direct problem is to find the scattered field $u^s(\cdot,\kappa) \in C^2(\Omega)\cap C(\overline{\Omega})$ such that the total field $u(\cdot,\kappa) = u^i(\cdot,\kappa)+u^s(\cdot,\kappa)$ is a solution of the Helmholtz equation

$$\Delta u(x,\kappa) + \kappa^2 u(x,\kappa) = 0 \quad \text{for } x \in \Omega. \tag{16}$$

Furthermore, the total field is required to satisfy the Dirichlet boundary condition

$$u(x,\kappa) = 0 \quad \text{for all } x \in \Gamma, \tag{17}$$

and the scattered field is supposed to be bounded in space, i.e.

$$|u^s(x,\kappa)| \leq c, \quad x \in \Omega, \tag{18}$$

for some constant $c > 0$ only depending on k. In the case that the wave number is a positive real number, we follow [4] and require the limiting absorbing principle, i.e. that for sufficiently small $\epsilon > 0$ the solution with wave number $\kappa = k_0 + i\epsilon$ exists and the pointwise limit

$$u(x, k_0 + i\epsilon) \longrightarrow u(x,k_0), \quad \epsilon \to 0, \tag{19}$$

is satisfied for every $x \in \Omega$.

Problem 2 (Direct Rough Surface Scattering Problem)**.** *Let $u^i(\cdot,\kappa)$ be an incident field due to a point source at the point $z \in \Omega$, i.e.*

$$u^i(\cdot,\kappa) = \Phi(\cdot,z,\kappa)\,. \tag{20}$$

Then, we want to find the total field $u(\cdot,\kappa) = u^i(\cdot,\kappa) + u^s(\cdot,\kappa)$, such that $u(\cdot,\kappa)$ solves the Helmholtz equation (16) and the Dirichlet boundary condition (17), the scattered part $u^s(\cdot,\kappa)$ satisfies the bound (18) and, for $\kappa > 0$, the limiting absorbing principle (19) is valid.

We can convert this scattering problem into a boundary value problem seeking the scattered field in the form

$$u^s(\cdot,\kappa) = v(\cdot,\kappa) - \Phi(\cdot,z',\kappa)\,. \tag{21}$$

Then, the Dirichlet boundary condition of the direct scattering problem with the incident field (20) yields

$$u^s(\cdot,\kappa) = -\Phi(x,z,\kappa) \text{ on } \Gamma,$$

and thus, the remainder v satisfies the boundary condition

$$v(x,\kappa) = \Phi(x,z',\kappa) - \Phi(x,z,\kappa) =: -G(x,z,\kappa)\,,\ x \in \Gamma\,. \tag{22}$$

We remark that the total field $u(\cdot,\kappa)$ satisfies the direct scattering problem if and only if $v(\cdot,k)$ solves the following boundary value problem, see [4]. Furthermore, the direct scattering problem can be reformulated in a well-posed integral equation, see [4],[5].

Problem 3 (Boundary Value Problem)**.** *Find $v(\cdot,\kappa) \in C^2(\Omega) \cap C(\overline{\Omega})$, which satisfies the Helmholtz equation (16), the boundary condition (22), the bound (18) and, for $\kappa > 0$, the limiting absorbing principle (19).*

The solvability of the frequency domain problem via a combined single- and double-layer approach for mildly rough surfaces has been shown in [4]. The authors first use Fourier arguments on a flat surface Γ_0. It is shown that the application of a single-layer potential on a flat surface with kernel

$$G_h(x,y) := \Phi(x,y) - \Phi(x,y - h\cdot e_3),\quad x,y \in \Gamma_0, \tag{23}$$

corresponds to multiplication with its Fourier transform

$$(FG_h(\cdot))(k) = \frac{1}{4\pi}\frac{(1 - e^{-h\sqrt{k^2-\kappa^2}})}{\sqrt{k^2-\kappa^2}},\quad k = |\boldsymbol{k}|. \tag{24}$$

Note that this is nonzero for h sufficiently small on $\boldsymbol{k} \in \mathbb{R}^2$ and that the function at $k = \kappa$ is bounded. The operator is boundedly invertible on the set of functions whose Fourier transform multiplied with $|\boldsymbol{k}|$ is square integrable, which corresponds to the solvability of the single-layer potential equation $S\varphi = f$ for $f \in H^1(\mathbb{R}^2)$.

For the reconstruction of U^s or u^s, respectively, on some test surface Γ^* (which we choose as a compactly perturbed plane as shown in Figure 2) we need to study the solvability of the single-layer boundary equation. This is carried out in the following result.

Theorem 1. *Consider the single-layer potential S with kernel G_h on a rough surface Γ^*. Then for h sufficiently small the operator is boundedly invertible as operator $L^2(\Gamma^*) \to H^1(\Gamma^*)$.*

Proof. The theorem is a direct consequence of the results of Lemma 3.3 and Theorem 3.4 in [5], where the density of the single-layer potential on a rough surface is explicitly estimated. □

4 A Time-Dependent Probe Method

Here, we first describe the field reconstruction problem in frequency domain, i.e. for measurements of the total field $u(\cdot,\kappa) = u^i(\cdot,\kappa) + u^s(\cdot,\kappa)$ for a single fixed wavenumber $\kappa > 0$ on a finite measurements plane $\Gamma_{h,A}$ with

$$\Gamma_{h,A} = \left\{x \in \mathbb{R}^3 : x_3 = h, |x_1| \le A, |x_2| \le A\right\} \tag{25}$$

for a constant $A > 0$ our task is to reconstruct $u^s(x,\kappa)$ in Ω. Note that we use the a-priori information $h > f_+$ to assure that there are no intersections between Γ_h and the unknown surface Γ.

Problem 4 (The Field Reconstruction Problem, frequency domain)**.** *Suppose we know the incident field $u^i(\cdot,\kappa) = \Phi(\cdot,z,\kappa)$ and the scattered field $u^s(\cdot,\kappa)$ on the plane $\Gamma_{h,A}$ for a fixed wavenumber κ with $\Im(\kappa) \ge 0$. We assume that the total field u satisfies the Dirichlet boundary condition $u = 0$ on the unknown surface Γ. Then, we try to find the total field and the surface Γ such that u is the solution of the direct problem (2) and $(u - u^i)(\cdot,\kappa)$ coincides with $u^s(x,\kappa)$ for all $x \in \Gamma_{h,A}$.*

We approximate the total field $u(\cdot,\kappa)$ via an single layer potential ansatz over some auxiliary surface $\Gamma^* \subset \overline{\Omega}$. For $\varphi \in L^2(\Gamma^*)$ the single layer potential is defined via

$$S\varphi(x,\kappa) := \int_{\Gamma^*} G(x,y,\kappa)\varphi(y)\, ds(y) \tag{26}$$

for all $x \in \mathbb{R}^3$. Here, the kernel G is the Dirichlet Green's function for the Helmholtz equation given by

$$G(x,y,\kappa) = \Phi(x,y,\kappa) - \Phi(x,y',\kappa)\,. \tag{27}$$

Let Λ_f be a surface given via (1). We define the projection operator for $B > 0$ by

$$P_B : \quad L^2(\Lambda_f) \to L^2(\Lambda_f) \tag{28}$$

$$\varphi(x) \mapsto \begin{cases} \varphi(x) & \text{if } \boldsymbol{x} \in [-B,B]^2\,, \\ 0 & \text{otherwise,} \end{cases} \tag{29}$$

where $x = (\boldsymbol{x}, f(\boldsymbol{x}))$. In particular, the restrictions of the measurements u^s on the plane $\Gamma_{h,A}$ can be seen as the image of the projection $P_A u^s \in P_A(L^2(\Gamma_h))$ of the scattered field u^s.

For the solution of the inverse problem we proceed as follows. We make the ansatz

$$u^s(\cdot,\kappa) = v(\cdot,\kappa) - \Phi(\cdot,z',\kappa) \tag{30}$$

and seek the projection $P_A v$ of the remainder v in a single layer potential, i.e.

$$P_A S\varphi(x,\kappa) = P_A v(x,\kappa) \text{ for all } x \in \Gamma_{h,A}\,. \tag{31}$$

Since $P_A S$ is a compact operator from $L^2(\Gamma^*) \to L^2(\Gamma_{h,A})$, see [1], equation (31) is ill-posed and we require some regularisation strategy.

To solve $P_A S\varphi(x) = P_A v(x)$ on $\Gamma_{h,A}$ we apply the *Tikhonov regularisation*, i.e. we solve

$$\alpha\varphi(\cdot,\kappa) + S^* P_A S\varphi(\cdot,\kappa) = S^* P_A v(\cdot,\kappa) \text{ on } \Gamma_{h,A}\,, \tag{32}$$

with a regularisation parameter $\alpha > 0$. In the following we indicate the dependence on the regularisation parameter $\alpha > 0$ by the subscript α. Then, we approximate the function v in the domain Ω^* above Γ^* via

$$v_\alpha(x,\kappa) = S\varphi_\alpha(x,\kappa)\,,\ x \in \overline{\Omega^*}\,. \tag{33}$$

Now, using the ansatz (30), we obtain an approximation u_α of the total field via

$$\begin{aligned} u_\alpha(\cdot,\kappa) &= u^i(\cdot,\kappa) + u^s_\alpha(\cdot,\kappa) \\ &= u^i(\cdot,\kappa) + S\varphi_\alpha(\cdot,\kappa) - \Phi(\cdot,z',\kappa) \\ &= S\varphi_\alpha(\cdot,\kappa) + G(\cdot,z,\kappa)\,. \end{aligned} \tag{34}$$

Algorithm 1 (Field Reconstructions)**.** *We reconstruct the time-dependent scattered field $U^s(x,t)$ by frequency-domain methods via the Fourier transform as follows:*

1. *For $\kappa \in \mathbb{R}$ evaluate $u^s(x,\kappa) := (\mathcal{F}U^s(x,\cdot))(\kappa)$, $x \in \Gamma_{h,A}$.*
2. *Reconstruct the scattered field $u^s = (u - u^i)(x,\kappa)$ for $x \in \Omega$ and $\kappa \in \mathbb{R}$.*
3. *Evaluate U^s via $U^s(x,t) = \mathcal{F}^{-1}u^s(x,\cdot)(t)$.*

Numerically we will employ a finite section version of the above approach, i.e. we study a single-layer potential defined on some finite part Γ^*_C of Γ^*. In the next section we will show convergence of this finite section method to the above solution for the infinite surface Γ^*.

We are now prepared to introduce the Time-Domain Probe Method, which relies on time-measurements of the scattered field $U^s(\cdot,t)$ on the measurement plane $\Gamma_{h,A}$. To this end we assume to know the measurements of the scattered field in time, that is

$$U^s(x,t) \text{ for all } x \in \Gamma_{h,A}\,, t \in \mathbb{R}. \tag{35}$$

Definition 2. *For a point $x \in \Omega$ we define the* first hitting time *with respect to the incident field U^i by*

$$T(x) := \inf\{t \in \mathbb{R} : |U^i(x,t)| > 0\}. \tag{36}$$

For $\boldsymbol{x} = (x_1, x_2) \in \mathbb{R}^2$ define

$$x_\lambda := (x_1, x_2, h - \lambda)\,,\ 0 < \lambda < h\,, \tag{37}$$

which is called a vertical needle. *Then the* first hitting parameter λ_* *is defined as*

$$\lambda_* := \sup_{x_\lambda \in \Omega} \lambda. \tag{38}$$

We use a grid of size $h_\lambda > 0$ for the discretization of the vertical probing, i.e. we employ

$$\lambda_\xi := h_\lambda \cdot \xi,\ \ \xi = 0, 1, 2, ... \tag{39}$$

Algorithm 2 (Time-Domain Probe Method)**.** *Let $U^s(x,t)$ be given for all $x \in \Gamma_{h,A}$ and $t \in \mathbb{R}$. To identify points $x \in \Gamma$ or to calculate a reconstruction f_{rec} for the surface height function f on Q, respectively, we choose a constant h_λ and $\epsilon = 2h_\lambda$ (where we assume wave speed $c = 1$) to carry out the following steps:*

1. *For every $\boldsymbol{x} \in Q$:*
2. *we successively investigate $\lambda = \lambda_\xi$ for $\xi = 0, 1, 2, ..$ given by (39):*
3. *with x_{λ_ξ} defined by (37) we reconstruct $U^s(x_{\lambda_\xi}, t)$ in the small interval $t \in (T, T+\epsilon)$ after the first hitting time $T = T(x_{\lambda_\xi})$ by the methods described in Algorithm 1.*
4. *If $|U^s(x_{\lambda_\xi}, t)| = 0$ for all $t \in (T, T+\epsilon)$, then we set $\mu(\lambda_\xi) = 0$ and conclude that $x_{\lambda_\xi} \in \Omega$. If there are points t such that $|U^s(x,t)| > 0$ in the time interval $(T, T+\epsilon)$, then we define $\mu(\lambda_\xi) = 1$ and we conclude that x_{λ_ξ} is close to Γ.*
5. *If $\mu(\lambda_\xi) = 1$ and $\mu(\lambda_\eta) = 0$ for all $\eta < \xi$, then we define the approximation*

   $$f_{rec}(\boldsymbol{x}) := h - \lambda \tag{40}$$

   to the unknown surface given by f.

To achieve a numerical algorithm we will employ a grid of points in the rectangle $Q = (a_1, b_1) \times (a_2, b_2)$. With n_1 or n_2 points in x_1 or x_2 direction, respectively, we use the notation

$$x_{1,j} = a_1 + \frac{b_1 - a_1}{n_1 - 1}(j-1),\ \ j = 1, ..., n_1 \tag{41}$$

$$x_{2,\ell} = a_1 + \frac{b_2 - a_2}{n_2 - 1}(\ell - 1),\ \ \ell = 1, ..., n_2. \tag{42}$$

We denote our horizontal grid by Q_{n_1,n_2}. For every point $\boldsymbol{x} \in Q_{n_1,n_2}$ we investigate the points x_{λ_ξ} for $\xi = 1, 2, 3, ...$ until $\mu(\lambda_\xi) = 1$. For the discrete version we need to make sure that we identify points which are close to the unknown boundary Γ. To this end we need to investigate appropriately chosen intervals $(T, T + \epsilon)$ depending on our discretization for simulations. Here, we have used a fixed $\epsilon = 0.2$ which was chosen by trial and error.

We will show convergence of the above algorithm in the next section.

5 Convergence of the Time-Domain Probe Method

The goal of this chapter to prove convergence of the Time-Domain Probe Method for the reconstruction of impenetrable rough surfaces.

As before we write U^s_α instead of U^s to indicate the dependence of the reconstructed scattered field U^s in the time-domain on the regularisation parameter $\alpha > 0$. From now on U^s is the true scattered field in the time-domain. We start with the investigation of convergence of U^s_α to U^s.

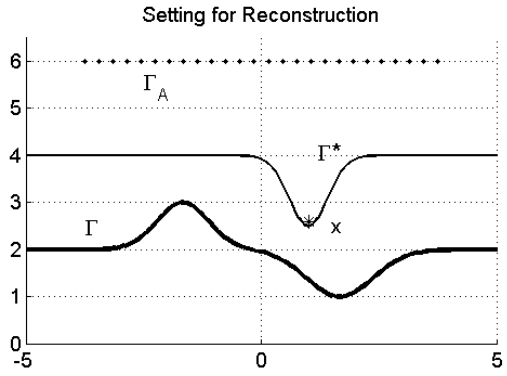

Figure 2: We show the setting for the reconstruction of the scattered field $U^s(x,t)$. The surface Γ^* is supposed to be in the domain Ω, i.e. above the unknown surface Γ. The measurement surface is Γ_A. The figure shows a point x in which $U^s(x,t)$ is reconstructed close to or on the boundary of the test surface Γ^*.

Theorem 3. *Consider the setting shown in Figure 2. Let U^i be an incident pulse and $U^s_{C,\alpha}$ the reconstructed field using the single-layer approach applied with the truncated surface*

$$\Gamma^*_C := \{x \in \Gamma^*, |x_1| \leq C\}. \tag{43}$$

If the test surface Γ^* is in Ω there exists a function $C_0(\alpha)$ with

$$C_0(\alpha) \to \infty, \quad \alpha \to 0 \tag{44}$$

such that for all $C(\alpha) \geq C_0(\alpha)$ *we obtain the convergence*

$$\left|U^s_{C,\alpha}(x,t)\right| \to |U^s(x,t)| \text{ for } \alpha \to 0, \tag{45}$$

for every x *above or on* Γ^*.

Proof. For $C = \infty$ we can choose $h > 0$ such that the single-layer equation $S\varphi = u^s$ from Γ^* onto $\Gamma_{h,A}$ has a unique solution in $L^2(\Gamma^*)$. In this case we obtain convergence of the reconstruction for a fixed frequency κ from the standard properties of the Tikhonov regularisation [23].

Denote the Tikhonov operator for Γ^* by R_α, i.e. $R_\alpha := (\alpha I + S^* P_A S)^{-1} S^* P_A$, and the Tikhonov operator arising from $S_C := SP_C$ based on Γ^*_C by R^C_α. In particular R^C_α is given by $R^C_\alpha := (\alpha I + P_C S^* P_A S P_C)^{-1} P_C S^* P_A$. Let φ_α be the regularized density for Γ^*, for which we know convergence $\varphi_\alpha \to \varphi$ towards the true solution φ on Γ^* for $\alpha \to 0$. Then, we have pointwise convergence

$$R^C_\alpha \to R_\alpha, \;\; C \to \infty \tag{46}$$

and thus

$$\varphi^C_\alpha := R^C_\alpha u^s \to \varphi_\alpha, \;\; C \to \infty. \tag{47}$$

This now shows that we have $\varphi^{C(\alpha)}_\alpha \to \varphi$ when $C(\alpha)$ is chosen appropriately. Finally, we remark that we obtain reconstructions with error estimates uniformly for compact intervals of frequencies with a norm of the inverse operator bounded by $C\kappa$ with some constant C, compare [5]. Since the fields are assumed to be in $C^3(\mathbb{R})$ with respect to time they decay proportional to κ^{-3} in frequency on the boundary and proportional to κ^{-2} in the domain Ω. Thus, applying the inverse Fourier transform we obtain convergence for the time-dependent fields as well. □

We base our arguments on the following basic properties of the wave equation [32].

Theorem 4 (Range of Influence)**.** *Let* D *be any subset of* Ω *and* $t > 0$. *Then, the values of any solution* $U^s(x,t)$ *in* D *of problem 1 depend only on the values of the total field* $U(x,s)$ *for* $s \in [0,t]$ *in the set*

$$D_t := \left\{ x \in \mathbb{R}^3 : \mathit{dist}(x,D) < t \right\}. \tag{48}$$

Proof. The statement is a consequence of the effects in hyperbolic equations to propagate along the characteristics of the equation, compare for example Theorem 14.1 in [32]. Here, the characteristics are the lines

$$|x - x_0| = t, \;\; t \geq 0 \tag{49}$$

shown in Figure 3 (a) and the domain D_t is the maximal domain from which points in D can be reached by an influence travelling along the characteristics in the time interval $[0,t]$. □

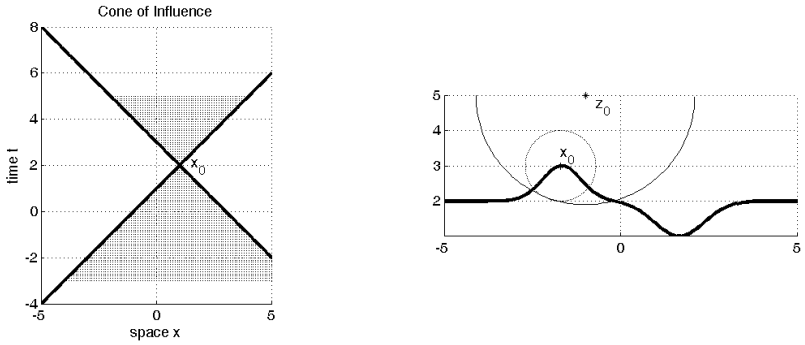

(a) (b)

Figure 3: We visualize the characteristics of the wave equation, where we used a wave speed $c = 1$. (a) The field at the point $x_0 = (1, 2)$ is influenced by the field in the dottet region below. It is influencing the field in the dotted cone above x_0. If the field is zero in the lower cone, then it must be zero at x_0. (b) Consider an incident field emerging from z_0 which reached x_0 at time T. The image shows the situation at $T + \delta T$, where the sphere of influence of the incident field is visualized by the large circle. The scattered field arising at T from x_0 can reach the sphere indicated by the dotted smaller circle.

Lemma 5. *Let U^i be an incident spherical pulse as given by (4) which is compactly supported in time. For every point $x \in \Omega$ we have that*

$$U^s(x,t) = 0 \text{ for all } t < T(x). \tag{50}$$

Proof. Consider the setting as visualized in Figure 3. The statement is a simple consequence of the fact that for a spherical pulse the total field $U(x,t)$ is zero in space-time range of influence of $(x, T(x))$. Thus, for $t < T(x)$ the scattered field $U^s(x,t)$ can never by positive in x. □

Theorem 6 (Convergence of Time-Domain Probe Method)**.** *The Time-Domain Probe Method as described in Algorithm 2 provides a complete reconstruction of the surface Γ above the rectangle Q in the sense that for $h_\lambda \to 0$ we have convergence*

$$f_{rec,h_\lambda}(\boldsymbol{x}) \to f(\boldsymbol{x}), \quad h_\lambda \to 0, \quad \boldsymbol{x} \in Q. \tag{51}$$

Proof. Assume that $x_\lambda \in \Omega$ above Q. Then according to Lemma 5 the scattered field $U^s(x_\lambda, t)$ is zero for $t < T(x)$ and since $U^i(x,t)$ is zero for $t < T(x)$ the same is true for the total field. Further, we want to show that $U^s(x,t)$ is zero even in a small neighbourhood $(T(x) - \epsilon, T(x) + \epsilon))$ of $T(x)$. Consider Figure 1, where the evolution of the field $U^s(x,t)$ is visualized. For any point $x \in \partial B_R$ with $x \in \Omega$ the influence arising from the incident field U^i needs some time $t > T(x)$ to reach $T(x)$. This is due to the triangle inequality which states that

$$|z_0 - \tilde{x}| + |\tilde{x} - x| > |z_0 - x| \tag{52}$$

for any point $\tilde{x} \in \Gamma$ and travel times are calculated by division of the distance by the wave speed c (where $T(x) = |z_0 - x|/c$). This proves that $\mu(\lambda) = 0$ for $x_\lambda \in \Omega$.

Now, consider a point $x_\lambda \in \Gamma$. Then we know that the scattered field satisfies $U^s(x,t) = -U^i(x,t)$ and by definition of the first hitting time $T(x)$ we know that in some interval $(T(x), T(x)+\epsilon)$ we have $|U^i(x,t)| > 0$. This proves that $\mu(\lambda) = 1$ for this case. Finally, from both cases and the setup of the needle search which is starting with $\lambda = 0$ we obtain convergence of the Time-Domain Probe Method. □

6 Numerical Study of the Time-Domain Probe Method

Our goal here is to show examples for the numerical realization for the Probe Method. We discretize the frequency interval $\mathbb{K} = [-\kappa_{max}, \kappa_{max}]$ using a step size $h_\kappa = \kappa_{max}/N$ with $2N$ frequency points. Our frequency grid it thus given by

$$\kappa_n = n \cdot h_\kappa, \quad n = -N, ..., N-1 \tag{53}$$

and we obtain a corresponding time grid by t_n by

$$t_n = n \cdot h_t, \quad n = -N, ..., N-1 \tag{54}$$

with time-stepsize h_t. The location of the point source for our simulation is $(-3, 0, 10)$ or $(0, 0, 13)$, respectively, and we choose $\sigma = 15$ or $\sigma = 4$, respectively, for the Gaussian pulse density. We use forward code developed by Heinemeyer, Lindner and Potthast [19] to calculate the scattered field in the time-domain $\boldsymbol{U}^s(x, t_n)$, $n = -N, ..., N-1$, for a selection of grid points x in the measurement patch $\Gamma_{h,A}$ at height $h = 10$, where we used $A = 5$.

For our numerical implementation we have realized a simplified version of the field reconstruction by a fixed choice of the auxiliary surface Γ^* below the unknown surface for the reconstruction of the scattered field u^s. We first calculate the frequency components by FFT from the time-domain measurements

$$\boldsymbol{u}^s(x, \kappa_n) = \mathcal{F}(\boldsymbol{U}^s(x, \cdot))(\kappa_n)\,, \quad n = -N, ..., N-1,\ x \in \Gamma_{h,A}\,. \tag{55}$$

Then, we reconstruct the scattered field $\boldsymbol{u}^s(x, \kappa_n)$ for $x \in \mathbb{Q} \subset \mathbb{R}^3$ where $\mathbb{Q}$ is a three-dimensional grid. For every fixed $x \in \mathbb{Q}$ we evaluate

$$\boldsymbol{U}^s(x, t_n) = \mathcal{F}^{-1}(\boldsymbol{u}^s(x, \cdot))(t_n)\,. \tag{56}$$

The second part of the numerical implementation is the probing procedure. We chose some fixed constant $\epsilon = 0.2$. For every point x in $\mathbb{Q}$ we evaluate the first hitting time $T(x)$ and investigate $U^s(x,t)$ for $t \in J := (T(x), T(x)+\epsilon)$. We set $\mu(x) = 1$ for those points for which $|U^s(x,t)| > \rho$ in J, where ρ is some numerical threshold which we use to discriminate $U^s(x,t) = 0$ and $|U^s(x,t)| > 0$.

We present simulations where the unknown surface consists of a hill and a valley. We use frequencies from 0 to 6 with a stepsize $h = 0.15$. In Figure 4 we presents a visualization

of the incident pulse in (a). The pictures (b), (c) and (d) show time slices of the scattered field at three different times t_1, ..., t_3. This confirms the arguments demonstrated in Figure 1.

The points which are identified as boundary points by the Time-Domain Probe Method are visualized in Figure 5. Figure (a) shows a slice plot along $x_2 = 0$. In (b) we show a horizontal view onto the reconstructions which proves that the location and height of the hill and valley are correctly found. Finally, a complete reconstruction of the height function is visualized in (c). The numerical results confirm the feasibility of the Time-Domain Probe Method.

The reconstructions here are comparable to frequency domain reconstructions for example by the point source method (c.f. [30], [31]) when we know and use the Dirichlet boundary condition. However, here we do not need to use this condition, so we are in a different setting where standard frequency domain algorithms do not work. A comparison to methods like the *range test* or the *no-response test* (compare [30]) needs to be part of future research.

Acknowledgements

The second author would like to thank both David Colton and Rainer Kress for numerous encouraging discussions about mathematics and much more over the last 15 years, for the continuing help and support and for their sustainable and wise attitude towards science and life in general.

References

[1] C. Burkard and R. Potthast, *Three-Dimensional Rough Surface Reconstruction by the Kirsch-Kress Method*, submitted for publication.

[2] A. Bamberger and T. Ha Duong, *Formulation Variationelle pour le Calcul de la Diffraction d'une Onde Acoustique par une Surface Rigide*, Math. Meth. in the Appl. Sci., **8** (1986), 598-608.

[3] S. N. Chandler-Wilde and C. Lines, *A Time Domain Point Source Method for Inverse Scattering by Rough Surfaces*, Computing, **75** (2005), 157-180.

[4] S. N. Chandler-Wilde, E. Heinemeyer and R. Potthast, *Acoustic Scattering by Mildly Rough Unbounded Surfaces in Three Dimensions*, SIAM J. Appl. Math, Volume **66**, Issue 3 (2006), 1001-1026.

[5] S. N. Chandler-Wilde, E. Heinemeyer and R. Potthast, *A Well Posed Integral Equation Formulation for the Three-Dimensional Rough Surface Scattering*, Royal Society of London Proceedings Series A, Volume **462**, Issue 2076 (2006), 3683-3705.

[6] S. N. Chandler-Wilde and P. Monk, *Existence, Uniqueness and Variational Methods for Scattering by Unbounded Rough Surfaces*, SIAM Journal on Mathematical Analysis, **37** (2005), 598-618.

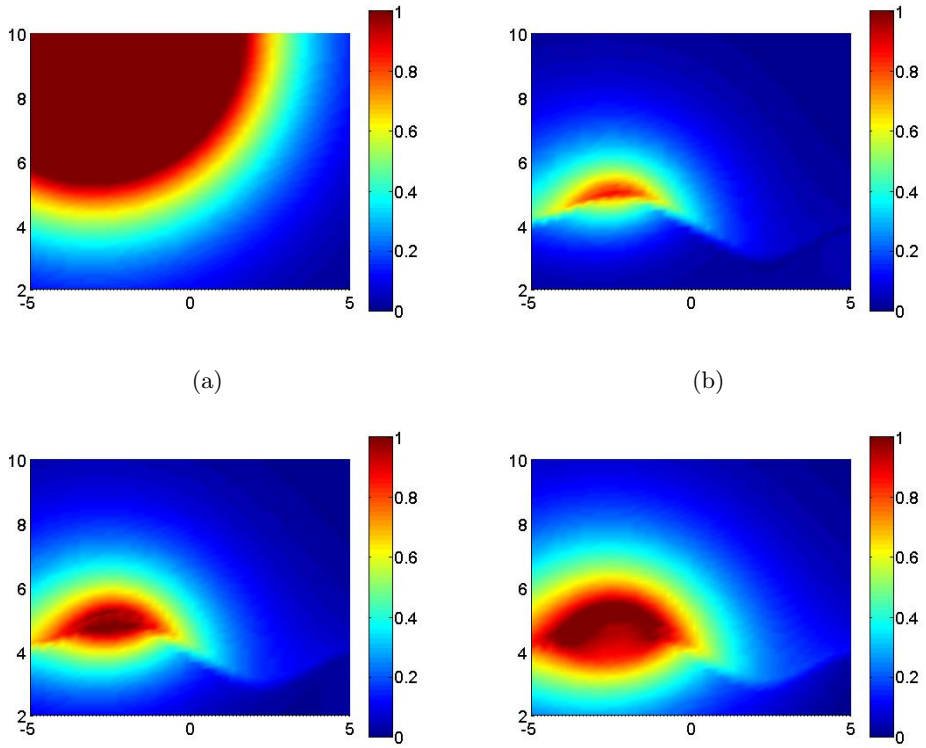

(a) (b)

(c) (d)

Figure 4: Figure (a) shows the modulus of an incident pulse arising from a source located in $z_0 = (-3, 0, 10)$ at some time t_1, where we cut values with $|U^s(x,t)| > 1$. In (b) we show the modulus of the scattered field which is arising when the pulse is touching the scattering surface above $(-3, 0)$. The yellow color denotes some threshold of $\rho = 0.6$ which might be used to detect the surface. Figures (c) and (d) show the time-dependent scattered field at two later times t_2 and t_3. The intersection of the expanding yellow line from (a) with the yellow areas from the scattered field move along the unknown surface Γ and are used by the Time-Domain Probe Method to reconstruct Γ.

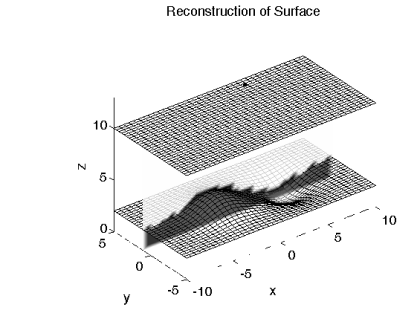

(a)

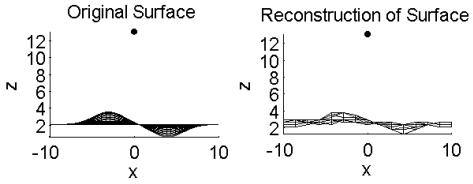

(b)

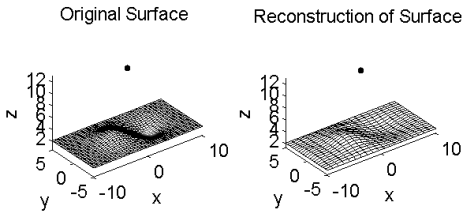

(c)

Figure 5: We show a selection of points which are identified by the Time-Domain Probe Method as being on or below the unknown surface Γ. In (a) we show reconstructions in one selected plane parallel to the x_1-x_3 plane. Measurements have been taken on the upper surface patch. The unknown surface is shown as a mesh, the points identified by the reconstruction method are colored black. (b) shows a side view onto the original and the reconstructed surface, the hill and valley are correctly identified. (c) demonstrates a complete reconstruction, where we applied some smoothing (convolution with a Gaussian kernel) before display of the reconstructed height function.

[7] S. N. Chandler-wilde and R. Potthast, *The Domain Derivative in Rough Surface Scattering and Rigorous Estimates for First Order Perturbation Theory*, Proceedings of the Royal Society London, **458** (2002), 2967-3001.

[8] S. N. Chandler-Wilde and C. R. Ross, *Scattering by Rough Surfaces: The Dirichlet Problem for the Helmholtz Equation in a Non-Locally Perturbed Half-Plane*, Mathematical Methods in the Applied Sciences, **19** (1996), 959-976.

[9] S. N. Chandler-Wilde and C. R. Ross, *Uniqueness Results for Direct and Inverse Scattering by Infinite Surfaces in a Lossy Medium*, Inverse Problems, **11** (1995), 1063-1067.

[10] S. N. Chandler-Wilde and B. Zhang, *Integral Equation Methods for Scattering by Infinite Rough Surfaces*, Mathematical Methods in the Applied Sciences, **26** (2003), 463-488.

[11] S. N. Chandler-Wilde and B. Zhang, *A Generalised Collectively Compact Operator Theory with an Application to Second Kind Integral Equations on Unbounded Domains*, Journal of Integral Equations and Applications, **14** (2002), 11-52.

[12] S. N. Chandler-Wilde, C. R. Ross and B. Zhang, *On the Solvability of Second Kind Integral Equations on the Real Line*, Journal of Mathematical Analysis and Applications, **245** (2000), 28-51.

[13] D. Colton and R. Kress, *Inverse Acoustic and Electromagnetic Scattering Theory*, 2. ed., Springer, Berlin, Heidelberg, 1998.

[14] F. Cakoni and D. Colton, *Qualitative Methods in Inverse Scattering Theory*, Springer, 2006.

[15] P. Davies and D. Duncan, *Stability and Convergence of Collocation Schemes for Retarded Potential Integral Equations*, SIAM J. Numer. Anal., **42** (2004), 1167-1188.

[16] J. A. DeSanto and R. J. Wombell, *Reconstruction of Rough Surface Profiles with the Kirchhoff Approximation*, Journal of the Optical Society of America A A-Optics Image Science And Vision, **8** (1991), 1892-1897.

[17] J. A. DeSanto and R. J. Wombell, *The Reconstruction of Shallow Rough-Surface Profiles from Scattered Field Data*, Inverse Problems, **7** (1991), L7-L12.

[18] J. Elschner and M. Yamamoto, *An Inverse Problem in Periodic Diffractive Optics: Reconstruction of Lipschitz Grating Profiles*, Appl. Anal., **81** (20) (2002), 1307-28.

[19] E. Heinemeyer, M. Lindner and R. Potthast, *Convergence and Numerics of a Multi-Section Method for Scattering by Three-Dimensional Rough Surfaces*, SIAM J. Numer. Anal, **46**, Issue 4 (2008), 1780-1798.

[20] M. Ikehata, *The Probe Method and its Applications*, In G. Nakamura, S. Saitoh, J.K. Seo and M Yamamoto, editors, Inverse Problems and Related Topics, Research Notes in Mathematics 419, CRC Press, London, 2000.

[21] S. Kusaik, R. Potthast and J. Sylvester, *A Range Test for Determining Scatterers with unknown Physical Properties*, Inverse Problems, **19** (2003), 533-547.

[22] A. Kirsch and N. Grinberg, *The Factorization Method for Inverse Problems*, Oxford Lecture Series in Mathematics and Its Applications, **36**, 2008.

[23] R. Kress, *Linear Integral Equations*, Springer Verlag, 1989.

[24] Ch. Lubich, *On the Multistep Time Discretization of Linear Initial-Boundary Value Problems and their Boundary Integral Equations*, Numer. Math., **67** (1994), 365-389.

[25] D. R. Luke and R. Potthast, *The Point Source Method for Inverse Scattering in the Time Domain*, Math. Meth. Appl. Sci., **29**, Issue 13 (2006), 1501-1521.

[26] A. Neubauer, B.Kaltenbacher and O. Scherzer, *Iterative Regularization Methods For Nonlinear Ill-Posed Problems*, Radon Series on Computational and Applied Mathematics, de Gruyter, 2008.

[27] R. Potthast, *Sampling and Probe Methods - An Algorithmical View*, Computing, **75** (2005), 215-235.

[28] R. Potthast, F. M. Fazi and P. A. Nelson, *Source Splitting via the Point Source Method*, submitted for publication.

[29] R. Potthast and J. Schulz, *From the Kirsch-Kress Potential Method via the Range Test to the Singular Sources Method*, Journal of Physics: Conference Series **12** (2005), 116 - 127.

[30] R. Potthast, *A Survey on Sampling and Probe Methods for Inverse Problems*, Topical Review for Inverse Problems, **22** (2006), R1-R47.

[31] R. Potthast, *Point-sources and Multipoles in Inverse Scattering*, Chapman & Hall, London, 2001.

[32] F. Treves, *Basic Linear Partial Differential Equations*, New York, 1975.